SUPPLEMENTAL MATERIAL

Reducing hypermuscularization of the transitional segment between arterioles and capillaries protects against spontaneous intracerebral hemorrhage

Short title: A novel mechanism of intracerebral hemorrhage

Authors

Julien Ratelade, PhD, Nicholas R. Klug, PhD[#], Damiano Lombardi, PhD[#], Monara Kaelle Servulo Cruz Angelim, PhD[#], Fabrice Dabertrand, PhD, Valérie Domenga-Denier, Rustam Al-Shahi Salman, PhD, Colin Smith, MD, Jean-Frédéric Gerbeau, PhD, Mark T. Nelson, PhD, Anne Joutel MD, PhD

Expanded Methods

Immunostaining of murine tissues

Primary antibodies to the following proteins were used: cleaved caspase 3 (1/1000, 9661; Cell Signaling, Danvers, MA, USA), aminopeptidase N (1/200, AF2335; R&D systems, Minneapolis, MN, USA), aquaporin 4 (1/250, sc-9888; Santa Cruz Biotechnology Dallas, Texas, USA), COL4A2 (1/200, clone H22; 7071, Chondrex Inc., Redmond, WA, USA), desmin (1/500, clone D33, M0760; DAKO, Glostrup, Denmark), desmin (1/500, ab8592; Abcam, Cambridge, UK), elastin (1/1000; from Dr. R. Mecham, Washington University School of Medicine, St. Louis, MO, USA), glial fibrillary acidic protein (GFAP) (1/10,000, clone GA5, MAB 360; Millipore, Temecula, CA, USA), GLUT1 (1/5000, 07-1401; Millipore), NG2 (1/250, AB5320; Millipore), NOTCH3 (1/2000, AF1308; R&D systems), perlecan (1/1000, clone A7L6, MAB1948P; Millipore), biotinylated perlecan (1/2000, clone A7L6, ab79465; Abcam), platelet derived growth factor receptor beta (PDGFR-β) (1/500, clone APB5, 14-402-82, ebioscience ThermoFischer Scientific, Waltham, MA,USA), FITC-conjugated α-SMA (1/2000, clone 1A4, F3777; Sigma Aldrich, St Louis, MO), smooth muscle myosin heavy chain (SMMHC) (1/500, BT-562; Biomedical technologies Inc., Stoughton, MA, USA), VE-Cadherin (1/100, clone 11D4.1, 550548; BD Pharmingen, San Jose, CA, USA).

The following secondary antibodies were used: Alexa Fluor-488–, Alexa Fluor-594– or Alexa Fluor-647–conjugated secondary antibodies (1/500; Life Technologies, Saint-Aubin, France).

We also used Alexa Fluor-633–conjugated hydrazide (1/2000, Life Technologies).

Mice were deeply anesthetized with sodium pentobarbital (80 mg/kg) and transcardially perfused with 25 mL of cold phosphate-buffered saline (PBS). The brain was removed, one hemisphere was fixed in 4% paraformaldehyde (PFA) for 1 hr at 4°C and cut into 100-µm-thick coronal sections using a vibratome, the other hemisphere was frozen and stored at -80°C until use. Eyes were collected and fixed in 4% PFA for 2 hrs at 4°C.

Dissected retinas were blocked in PBS containing 5% bovine serum albumin (BSA) and 0.2% Triton at room temperature (RT) for 2 hrs. Sections were then incubated for 24 hrs at 4°C with primary antibodies diluted in PBS containing 0.5% BSA, 0.2% Triton and with secondary antibodies diluted in the same buffer. Free floating 100-µm-thick sections were blocked in PBS containing 10% fetal calf serum (FCS) and 0.5% Triton at RT for 2 hrs.

Sections were then incubated for 24 hrs at RT with primary antibodies diluted in PBS containing 1% FCS, 0.5% Triton and with secondary antibodies diluted in the same buffer. Methanol & acetone fixed cryosections (20-µm-thick) were blocked in PBS containing 5% FCS and 0.1% Triton at RT for 2 hrs. Sections were then incubated for 24 hrs at RT with primary antibodies diluted in PBS containing 0.5% FCS, 0.1% Triton and with secondary antibodies diluted in the same buffer.

Brain sections were imaged with a confocal spinning disk CSU-W1 mounted on a Leica DMI8 microscope (Leica Microsystems, Nanterre, France). Brain or retinal vessels were imaged with a TCS SP5 or SP8 laser-scanning confocal microscope (Leica Microsystems). Retinas were imaged using an epifluorescence Eclipse 80i microscope (Nikon, Champigny sur Marne, France) or an Axio Observer Z.1 Wildfield Fluorescence microscope (Zeiss, Oberkochen, Germany).

EdU labeling of proliferating cells

For detection of proliferating cells in vivo, a stock of 1 mg 5-ethynyl-2deoxyuridine (EdU) (Sigma) was dissolved in 10µl DMSO plus 90µl PBS; 10µl of this stock solution per gram of body weight were injected intraperitoneally 4 hours before the animals were sacrificed and transcardially perfused with PBS. Retinas were collected and processed as described above. EdU-positive cells were detected with the Click-iT EdU Alexa Fluor-647 Imaging Kit (ThermoFisher Scientific***).***

Perl's staining

Mice were deeply anesthetized with sodium pentobarbital (80 mg/kg) and transcardially perfused with PBS. The brain was removed, fixed in 4% PFA overnight and cut into 100-µm-thick sagittal sections using a vibratome. Sections were incubated in a 2% hydrochloric acid/2% potassium ferrocyanide solution for 10 minutes and were imaged using a microscope-mounted Nikon DXM1200 digital camera. Between 22 and 24 sections, spaced 200 µm apart and spanning the whole brain, were analyzed per mouse for ICH counting.

Immunostaining of human brain sections

Paraffin embedded tissues from 7 controls and 7 patients with deep ICH were used for histopathological studies. The demographic information of all cases is provided in Supplementary Table 3. Paraffin embedded 7 µm-thick sections were stained according to standard protocols. Primary antibody against α-SMA (1/500, clone 1A4, M0851, DAKO,

Glostrup, Denmark) was added in blocking solution and incubated overnight at 4°C. Secondary biotinylated antibody (1/100, Vector laboratories, Burlingame, CA) was subsequently incubated for 2 hours (RT). Immunoreactivity was visualized with avidin/biotin-horseradish peroxydase complex (Vectastain ABC-HRP kit, Vector Laboratories) and developed with 3,3'-diaminobenzidine (Sigma Aldrich). Sections were imaged using a Zeiss Axioplan 2 microscope (Carl Zeiss). 75 transversely cut arterioles/transitional segments located in the basal ganglia were analyzed per individual.

Quantitative analysis

All quantifications were performed using ImageJ (https://imagej.nih.gov/ij/) and all procedures were performed with prefixed parameters under blinded conditions.

Arteriolar smooth muscle cell loss. Quantification was performed on flat-mounted retinas labeled for α-SMA, NG2, perlecan and DAPI. Epifluorescence images were obtained using a 10X objective (2560 x 2160 pixels/images, 0.65 µm/pixel, 11 bits) and a mosaic image of the whole retina was reconstructed. Arteriolar segments within a 1.5-mm radius centered on the optic nerve were visually inspected for gaps in α-SMA labeling. The length of arteriolar segments with gaps as well as the total length of arteriolar segments was measured (1 retina/mouse). Results are expressed as the percentage of the arteriolar bed containing gaps.

Number of mural cells in transitional segments (TS) in adult retina. Quantification was performed on images of whole retinas labeled for α-SMA, NG2, perlecan and DAPI. TS were identified as segments positive for α-SMA and with mural cell nuclei bright for NG2. Mural cell nuclei were counted and the length of the TS was measured. Between eight and ten TS located in the periphery of the retina were quantified per mouse. Data are reported as a number of cells per mm.

Pericyte density and coverage. Quantification was done on retinas labeled for α-SMA, NG2 perlecan, and DAPI. At least five fields (906 x 874 µm) containing mainly capillaries and located in the periphery of the retina were used for quantification. All three channels (α-SMA, NG2, perlecan) were treated with Gaussian Blur filter and separately segmented using Otsu's thresholding. For NG2 staining, background (rolling ball tool) was subtracted before thresholding. α-SMA-positive blood vessels were removed using the Image Calculator plugin and veins were manually erased using the rubber tool to keep only capillaries. For pericyte coverage, segmented NG2 and perlecan pictures were combined using the Image Calculator command AND and the surface of NG2 staining within perlecan-positive vessels was

measured and reported as a percentage. Pericyte density was determined by counting the number of NG2-positive cell bodies within the field and measuring the total length of capillaries using the skeletonize plugin on the segmented perlecan picture. Data are reported as a number of cells per mm.

Mean fluorescence intensity of α-SMA in TS from adult mice. Quantification was done on images of whole retinas stained for α-SMA, NG2, perlecan and DAPI. A circle of 1.65 mm radius centered on the optic nerve was drawn and fluorescence within the circle was removed. The vessels positive for α-SMA outside this circle were mainly TS as seen by the presence of mural cell nuclei bright for NG2 and were used for quantification. Images with the α-SMA staining were background-subtracted using the rolling ball tool and thresholded to isolate areas positive for α-SMA. These areas were assembled using the analyze particle tool to create a mask. The mask was applied to the original α-SMA picture and the mean fluorescence intensity was measured. Data are reported as normalized values to the mean of the control group.

In the brain, quantification was done on 100-µm-thick vibratome sections stained for α-SMA, desmin, perlecan and DAPI. Z-stack confocal images covering the whole thickness of the section were obtained using a 10X objective (z-step = 6 µm, 1638 x 1638 pixels/images, 0,7 µm/pixel, 16 bits). Cortex, thalamus and striatum were scanned (9 z-stacks per section) and one single mosaic image was reconstructed. Maximum intensity projection pictures were used for quantifications. Arterioles (low for desmin) were manually removed from the picture using the rubber tool to keep only TS. Mean fluorescence intensity was measured using the macro described above on 10 sections per brain.

Mean fluorescence intensity of α-SMA in retinal TS and length of retinal arterioles or TS from P10 or P23 mice. Quantification was done on images of whole retinas stained for α-SMA, NG2 and DAPI. Arterioles were identified as α-SMA^{high} vessels. TS were identified as collateral branches with a diameter comprised between 8-11 µm that were covered by rounded NG2^{high}, α-SMA^{low} mural cells. α-SMA-stained vessels were background-subtracted using the rolling ball tool and thresholded to isolate areas positive for α-SMA. Then arterioles were manually erased using the polygon tool and a mask corresponding to TS was created. This mask was applied to the original α-SMA image for measurement of the mean fluorescence intensity; data are reported as normalized values to the mean of the control group.

A segmented line was drawn over α-SMA-stained vessels for length measurement. Each retina comprises an average of 5-6 arterioles and 32-61 TS (P10), 72-105 (P23). Data are reported as normalized values to the area of retina.

Proliferation of mural cells. Quantification was done on images of whole retinas stained for α-SMA, NG2, EdU and DAPI. Arterioles and TS were identified as described above and EdU positive nuclei within α-SMA- and NG2-positive cell bodies were manually counted. In arterioles, nuclei of SMC were further distinguished from those of endothelial cells based on their shape: rounded for SMC and elongated for endothelial cells. Data are reported as normalized values to the area of retina.

Arteriole/TS remodeling in human brains. Analyses were conducted on paraffin sections of microvessels located in the basal ganglia. For ICH patients, we used brain tissue from the hemisphere contralateral to the hemorrhage. Quantifications were done on bright field images acquired with a 40X objective (1392 x 1040 pixels/image, 0.16 µm/pixel, 16 bits). Cross-sectional profiles of randomly selected TS/arterioles (n=525/group) were analyzed. For each vessel, the area stained for α-SMA (α-SMA + area), which corresponds to the media, and the area of the lumen were obtained using automatic segmentation. Vessel diameter was estimated using the following formula $d = 2 \times \sqrt{(\text{Lumen area}/\pi)}$. Data are presented as the ratio of the media area to the lumen area.

Intracerebral hemorrhages. ICHs were counted on Perl's-stained brain sections. Fresh ICHs were visualized by the presence of blood and old ICHs by the presence of dark blue hemosiderin deposits. Between 22 and 24 100-µm-thick sections, spaced 200 µm apart and spanning the whole brain were analyzed per mouse.

Vascular reactivity in pressurized retina explants

Following brain removal, the entire eye and surrounding tissue was dissected using angled eye scissors. Eyes were placed on ice cold calcium free artificial cerebrospinal fluid (aCSF) (in mM: 125 NaCl, 3 KCl, 2 $MgCl_2$, 4 Glucose, 26 $NaHCO_3$, and 1.25 NaH_2PO_4) which was bubbled with 95% O_2 and 5% CO_2, pH 7.4. Bones, muscles, and surrounding nervous tissue were removed with eye scissors (bone), fine forceps and Vannas spring scissors in a small silicone coated dissecting dish containing bubbled ice cold calcium free aCSF. The ophthalmic artery, surrounding connective tissue and a section of optic nerve was left intact for cannulation. Branches of the ophthalmic artery which did not lead to the central retinal artery were ligated using fine suture. Once the cornea, lens and sclera were removed (a small

sclera patch around optic nerve was left intact to avoid damaging the central retinal artery), the retina and attached nerve and ophthalmic artery were moved to an arteriography perfusion chamber (Living Systems Instrumentation, Inc) containing a silicone platform with bubbled ice cold calcium free aCSF. The ophthalmic artery was cannulated using a glass micropipette filled with aCSF (in mM: 125 NaCl, 3 KCl, 2 $CaCl_2$, 1 $MgCl_2$, 4 Glucose, 26 $NaHCO_3$, and 1.25 NaH_2PO_4). Using the micromanipulator attached to the cannula, the retina was positioned over the silicone platform and cut into four equal leaves. The retinal leaves were pinned to the platform and the cannula was moved below (in a notch cut from the platform) so that the retinal mount was flat and superficial vasculature was facing upwards. The chamber was then perfused at 5 ml/min with 37 ºC bubbled aCSF. The cannula was attached to a pressure sensor and gravity fed aCSF at a 40mmHg pressure. Wash away of red blood cells and simultaneous dilation of arterioles confirmed pressure in arteries.

The retina was allowed to equilibrate in bath perfusion at 40 mmHg for 30 min. The diameter of TS located in the periphery of the retina was recorded using transmitted light and a water dipping 40X objective (NA 0.8) mounted on a Nikon Eclipse 600 microscope equipped with a brightfield DIC filter and a EMCCD camera (Andor, Belfast, UK). In a subset of experiments the response to a rapid pressure increase from 40 mmHg to 80 mmHg at the ophthalmic artery (raising the pressure column in ~5 sec) was performed to determine pressure-induced constriction. Agonist and high K+ induced constriction was determined by increasing concentrations of the thromboxane mimetic U-46619 (10 to 100 nM) (Cayman Chemical, Ann Arbor, MI, USA) or adding 60 mM KCl (iso-osmotic by Na+ substitution) solution to the chamber perfusion aCSF solution. Constriction response of transitional segment was calculated with the following formula: 100 * (initial diameter – diameter after drug, high K+, or 80 mmHg) / initial diameter. Three measures at different locations were done for each TS and averaged.

Isolation of cerebral microvessels

Brain tissue was homogenized in 20 mL of cold Minimum Essential Medium (MEM) (Thermofisher scientific) with 20–40 up-and-down strokes in a glass homogenizer. Homogenate was mixed with an equal volume of cold MEM containing 35% Ficoll PM400 (Sigma Aldrich). The suspension was then centrifuged at 6000*g* for 20 min at 4°C. The supernatant was discarded and the pellet was resuspended in PBS containing 1% BSA. The suspension was then triturated and poured through a 100 μm nylon mesh to remove large

vessels. The flow-through was then poured on a 40 µm nylon mesh. Microvessels retained on the nylon mesh were collected in PBS by inversion of the nylon mesh and pelleted by centrifugation. Purity of microvessel preparations was monitored by phase-contrast microscopy and immunostaining for vessel, neuronal and glial cell markers. For immunofluorescence, vessels retained on the 100 µm and 40 µm nylon meshes were collected in PBS by inversion of the nylon mesh and allowed to adhere on a Lab-Tek chamber slide (Sigma Aldrich). Immunofluorescence was performed as described above.

Dissection of brain arteries.

Pial arteries were dissected under scope and frozen in liquid nitrogen until use.

RNA preparation and quantitative reverse transcription-polymerase chain reaction (qRT-PCR) analyses.

Isolated cerebral microvessels or pial arteries were homogenized on ice in SV RNA lysis buffer (Promega, Madison, WI, USA) using a polytron homogenizer, and total RNA was extracted following the manufacturer's protocol (SV Total RNA Isolation System; Promega). cDNA was synthesized from total RNA using M-MLV reverse transcriptase (ThermoFisher Scientific). Quantitative PCR was performed on a CFX Connect Real-Time PCR detection system (Bio-Rad, Oxford, UK) using SYBR Green PCR master mix (Bio-Rad). The primer pairs used are listed in Supplementary Table 1. Results are presented as β-actin–normalized relative expression levels.

Blood pressure measurement

Blood pressure was non-invasively measured by determining the tail blood volume with a volume pressure recording sensor and an occlusion tail-cuff (CODA System; Kent Scientific Corporation, Torrington, CT). Mice were placed in warmed restraining chambers and acclimatized to the experimental procedure for 2 weeks before data acquisition. Three independent measures were recorded per animal and averaged.

Mathematical model

A mathematical model describing hemodynamics in a human retinal arteriolar network was written as described previously[30]. The 3D geometry used was a human retinal network segmented by exploiting standard fundus camera images. The blood flow was described using incompressible Navier-Stokes equations. The endothelium mechanics was described by shell equations (non-linear Koiter without bending) and mural cells by a distribution of 1D elastic

fibers attached to the endothelium. With respect to the work presented previously[30,31], there were two main modifications of the model. First, the density of the fibers was not uniform. Here different densities were considered to implement SMC loss in arterioles and hypermuscularization in TS (values are shown in Fig 7B). Moreover, the terminal 3-elements Windkessel models used to impose the boundary conditions and render the missing part of the network were tuned to account for the level of muscularization (hyper-muscularization induces a decrease in vessels radius hence increasing the resistances of the Windkessels and decreasing the capacitance). The weak formulation of the equations was written and the discretization was performed by using standard finite elements.

Expanded results

Col4a1$^{+/G1064D}$ mutant mice develop spontaneous deep ICH and similar microvascular changes in the retinal and brain vasculature

The G498V mutation is located in the cyanogen bromide-derived fragment CB3[IV] of COL4A1, known to contain several integrin-binding sites[46]. Hence, we wondered whether microvascular changes observed in *Col4a1$^{+/G498V}$* mice were specific to this mutation or common to pathogenic mutations in the COL4A1-disease. To address this issue, we analyzed *Col4a1$^{+/G1064D}$* mice, a mouse line produced by N-ethyl-N-nitrosourea mutagenesis [21]. Previous works have shown that *Col4a1$^{+/G1064D}$* mice develop spontaneous ICH, kidney lesions characterized by glomerular cysts and tubular defects as well as eye defects including anterior segment dysgenesis[21-23]. The G1064D mutation is located in the central collagenous domain of COL4A1 and mutates a glycine residue in one of the Gly-Xaa-Yaa amino acid repeats which are crucial for proper folding of the type IV collagen triple-helix. This mutation is associated with decreased secretion of collagen type IV to basement membranes[22].

We found that *Col4a1$^{+/G1064D}$* mice had a 28% perinatal lethality, and 92% of mutant mice had developed spontaneous deep ICH at 3 months of age (Fig. S10 A-B). In comparison, the G498V mutation did not affect viability at least until 6 months of age and penetrance of ICH was near 20 % in 3-month-old *Col4a1$^{+/G498V}$* mice[14]. Immunostaining of flat-mounted retinas from 3-month-old *Col4a1$^{+/G1064D}$* mice showed prominent SMC loss in arterioles (10.6 $\pm$ 5.6 %) (Fig. S10 C, E) and robust hypermuscularization of TS with a higher number of mural cells and increased α-SMA expression (33.7 $\pm$ 13.1 %) (Fig. S10 D, F). In comparison,

Col4a1$^{+/G498V}$ mice at 3 months of age had 2.7 ± 2.6 % (ranging from 0.3 to 7.6%) SMC loss in arterioles[7] and 11.9 ± 7.1 % increase in α-SMA expression in the TS (Fig S6).

Analysis of brain vessels using high resolution confocal imaging revealed similar loss of SMCs in arterioles and hypermuscularization of TS in *Col4a1*$^{+/G1064D}$ mice (Fig. S11). Together these data indicate that *Col4a1*$^{+/G1064D}$ mice exhibit similar pathology than *Col4a1*$^{+/G498V}$ mice, although more severe, and suggest that the combination of SMC loss in arterioles and hypermuscularization of TS are common microvascular changes in the COL4A1 disease.

Expanded discussion

Excessive muscularization of the TS in a broader context

Ablation of astrocytic laminin in the mouse also leads to spontaneous deep ICH in adult mice[47]. Strickland and colleagues reported that the lack of astrocytic laminin disrupted integrity of arteriolar SMC and vessel wall, but remarkably upregulated the expression of α-SMA and SM22 in capillary pericytes[47,48]. However, eyeing up the morphology of these "α-SMA positive capillary pericytes" (figure 8a from Yao et al[48]), we suspect that these are TS with excessive muscularization, although this awaits experimental confirmation, hence leading us to speculate that ICH secondary to ablation of astrocytic laminin arises from the same zonation of microvascular pathology.

Experimental studies have established that chronic arterial hypertension can produce mural cell hyperplasia or hypertrophy, especially in the large cerebral arteries [49]. Yet, the potential role of chronic hypertension in hypermuscularization of brain TS remains to be investigated. However, although high blood pressure is the strongest modifiable risk factor for deep ICH, it is just one of the drivers. Interestingly, 3 out of the 7 patients we have analyzed had no known history of chronic hypertension although data on cardiac or renal pathology, which may have supported a normotensive status, were not available in these patients due to limited post-mortem examinations. Thus, it is conceivable that other risk factors, including genetic variants, play a role in the microvascular pathology. In this respect, it is remarkable that an intronic variant in the COL4A2 locus, with a potential regulatory effect, increases the risk for deep ICH[50,51].

Supplementary Figures

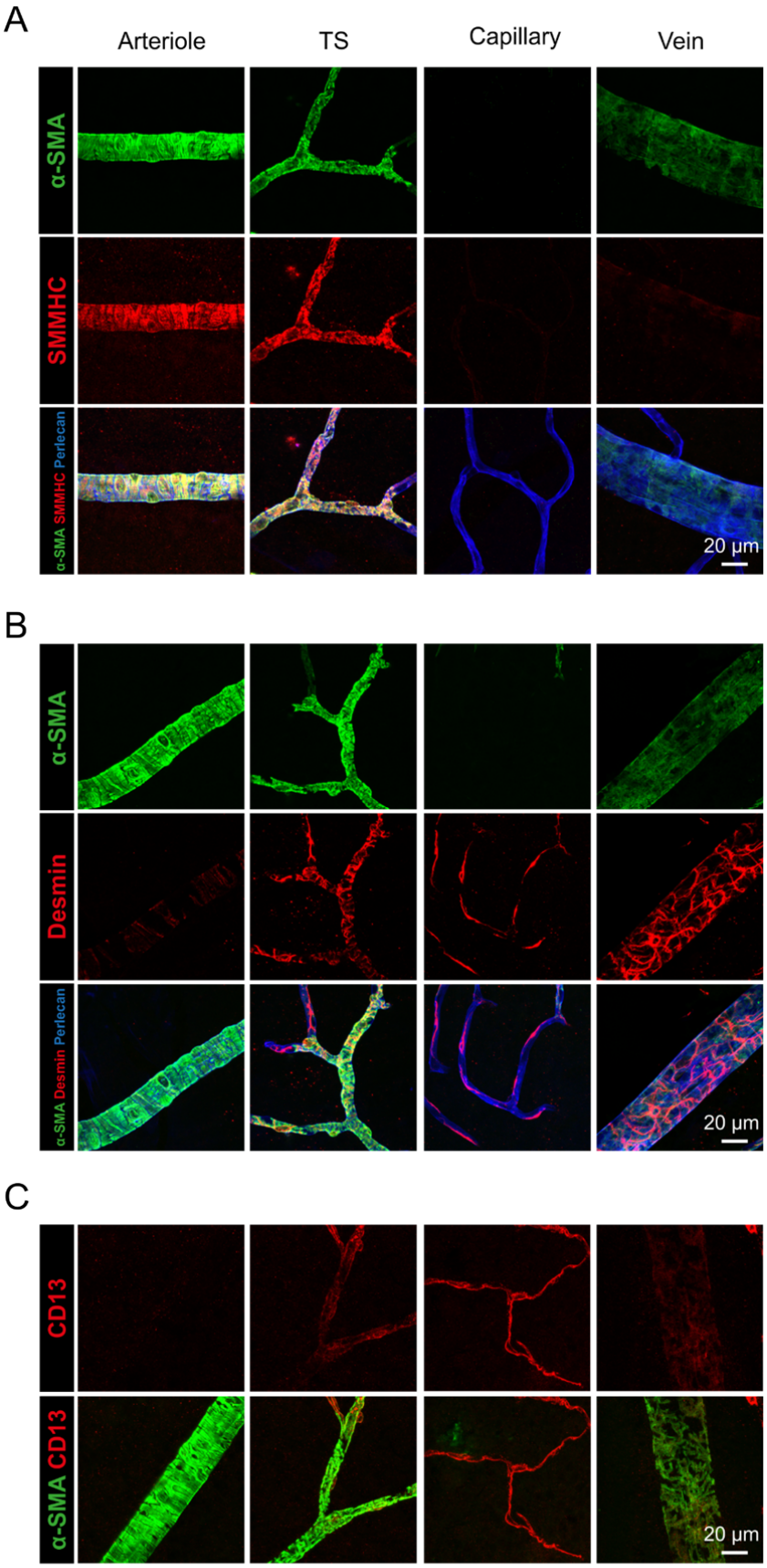
A
Arteriole
TS
Capillary
Vein
α-SMA
SMMHC
α-SMA SMMHC Perlecan
20 μm
B
α-SMA
Desmin
α-SMA Desmin Perlecan
20 μm
C
CD13
α-SMA CD13
20 μm

Figure S1

Figure S1. Heterogeneity of mural cells in retinal vessels.

A-C. Representative confocal pictures of adult mouse retina stained for α-SMA, perlecan and SMMHC (**A**), desmin (**B**) or aminopeptidase N/CD13 (**C**). Scale bar: 20 µm.

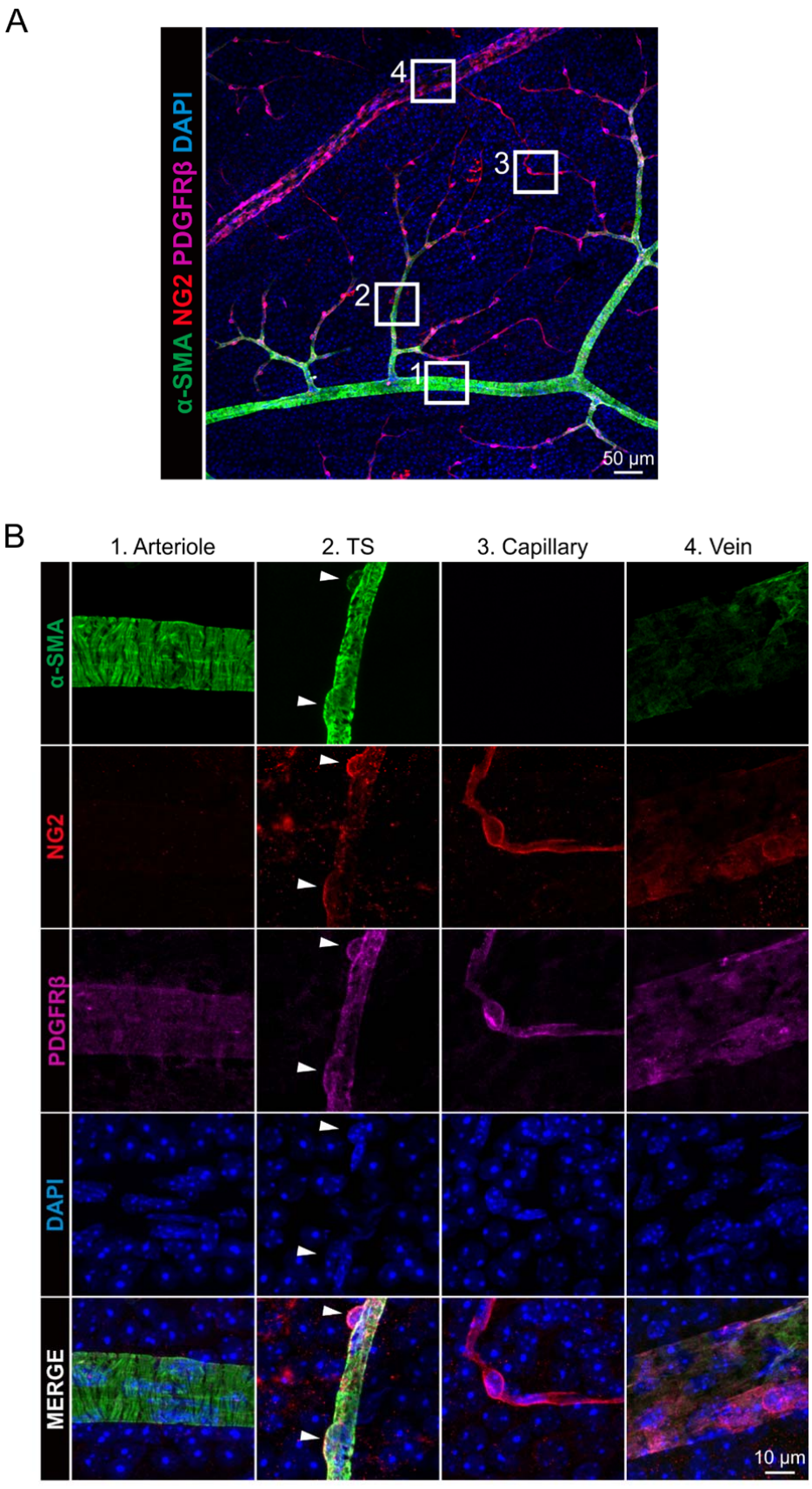
A
α-SMA NG2 PDGFRβ DAPI
4
3
2
1
50 µm
B
1. Arteriole
2. TS
3. Capillary
4. Vein
α-SMA
NG2
PDGFRβ
DAPI
MERGE
10 µm

Figure S2

Figure S2: Expression of PDGFR-β and NG2 in the retinal vasculature.

A-B. Representative confocal pictures of adult mouse retina stained for α-SMA, NG2, PDGFR-β and DAPI. **A**. Low magnification view of the retinal vasculature. **B**. Higher magnification pictures of the boxed regions numbered in A, showing SMCs in arterioles (1), transitional cells in TS (2), pericytes in capillaries (3) and SMCs in veins (4). Arrowheads show protruding cell body of transitional cells that contain the nucleus, where NG2 staining is mostly concentrated. Scale bars: 50 μm (A) and 10 μm (B).

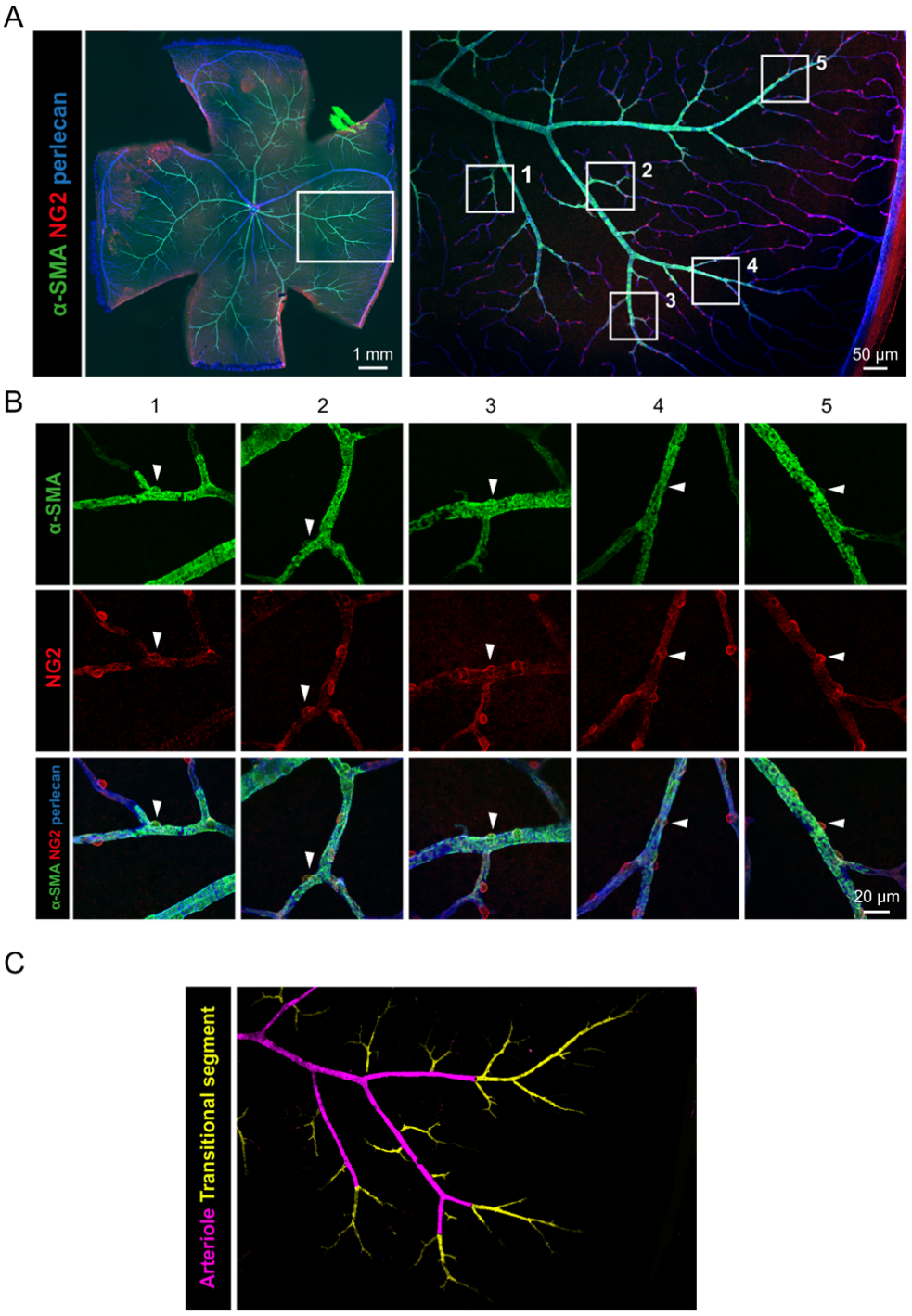

Figure S3

Figure S3. Location of transitional segments in the retinal vasculature.

A-B. Representative confocal pictures of adult mouse retina stained for α-SMA, NG2 and perlecan. **A**. Whole flat mounted retina (left) and higher magnification view of the white boxed region in A (right). **B**. Higher magnification pictures of the boxed regions numbered in A-right showing TS, covered by mural cells expressing α-SMA and NG2 with protruding cell

nuclei (arrowheads), at every arteriole/capillary transition. **C**. Schematic of the location of arterioles (pink) and TS (yellow) on the retinal vascular tree in A-right. Scale bars: 1 mm (A, left), 50 μm (A, right) and 20 μm (B).

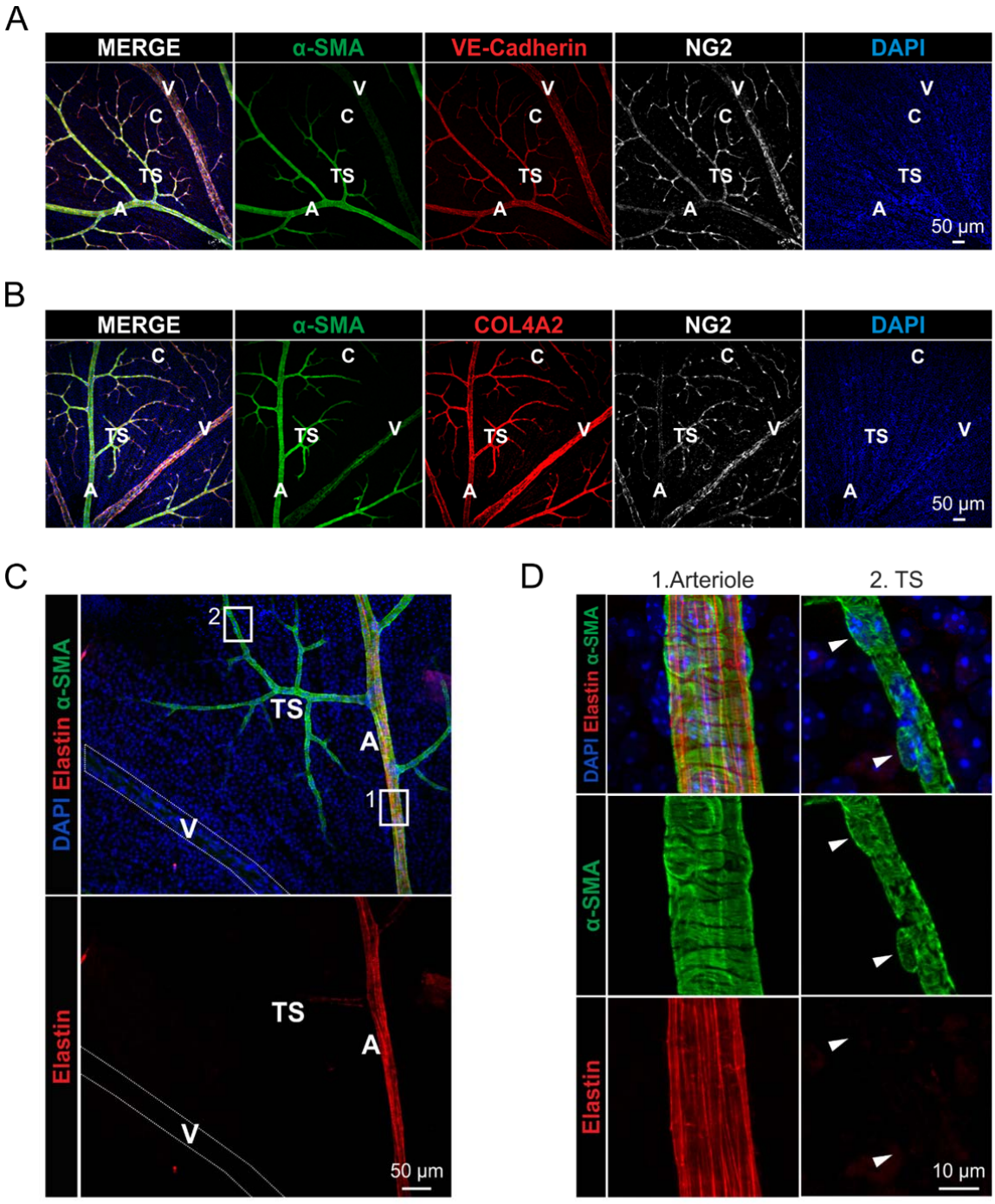

Figure S4

Figure S4: Expression of VE-cadherin, COL4A2 and elastic fibers in the retinal vasculature.

A-B. Representative confocal pictures of adult mouse retina immunostained for α-SMA, NG2, DAPI and VE-cadherin (**A**) or COL4A2 (**B**) showing VE-cadherin and COL4A2 expression in arterioles (A), transitional segments (TS), capillaries (C) and veins (V). **C.** Confocal

pictures of adult mouse retina immunostained for α-SMA, elastin and DAPI showing elastin expression in arterioles (A) but not in TS, capillaries and veins (V). **D.** Higher magnification pictures of the boxed regions shown in C. Arrowheads point to nuclei of transitional cells of TS. Scale bars: 50 μm (A, B, C) and 10 μm (D).

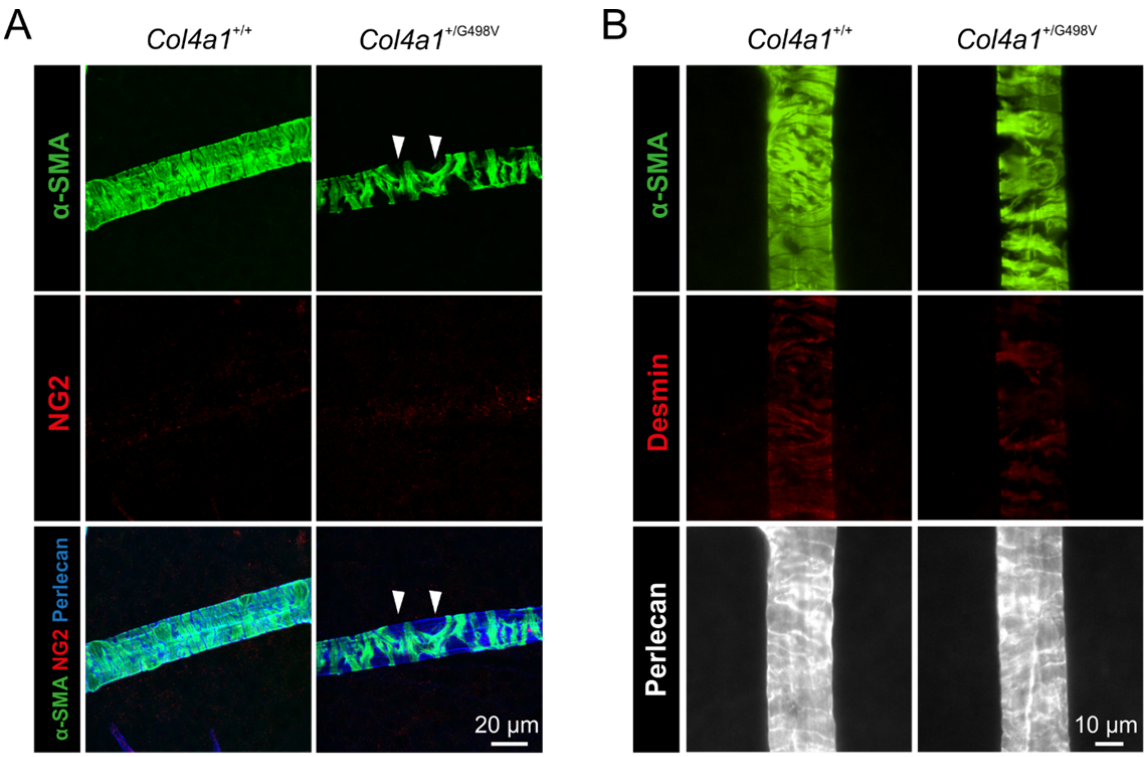

Figure S5

Figure S5. SMC loss in retinal arterioles of *Col4a1*$^{+/G498V}$ mice.

A-B. Representative pictures of retinal arterioles from *Col4a1*$^{+/+}$ and *Col4a1*$^{+/G498V}$ mice aged 6 months stained for α-SMA, perlecan and NG2 (A) or desmin (B), showing SMC loss in mutant arterioles (arrowheads). Scale bars: 20 µm (A) and 10 µm (B).

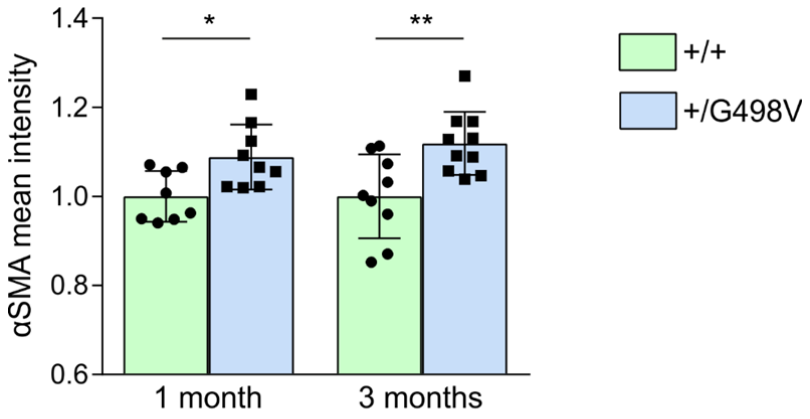

Figure S6

Figure S6. Hypermuscularization of TS is detected as early as one month of age in *Col4a1*$^{+/G498V}$ mice.

Quantification of α-SMA mean fluorescence intensity in retinal TS of *Col4a1*$^{+/+}$ and *Col4a1*$^{+/G498V}$ mice at 1 month (n=8 +/+ and 9 +/G498V mice) and 3 months (n=9 +/+ and 10 +/G498V mice). Data were analyzed by 2-way ANOVA and Bonferroni's multiple comparison test. * P=0.0431, ** P=0.0033.

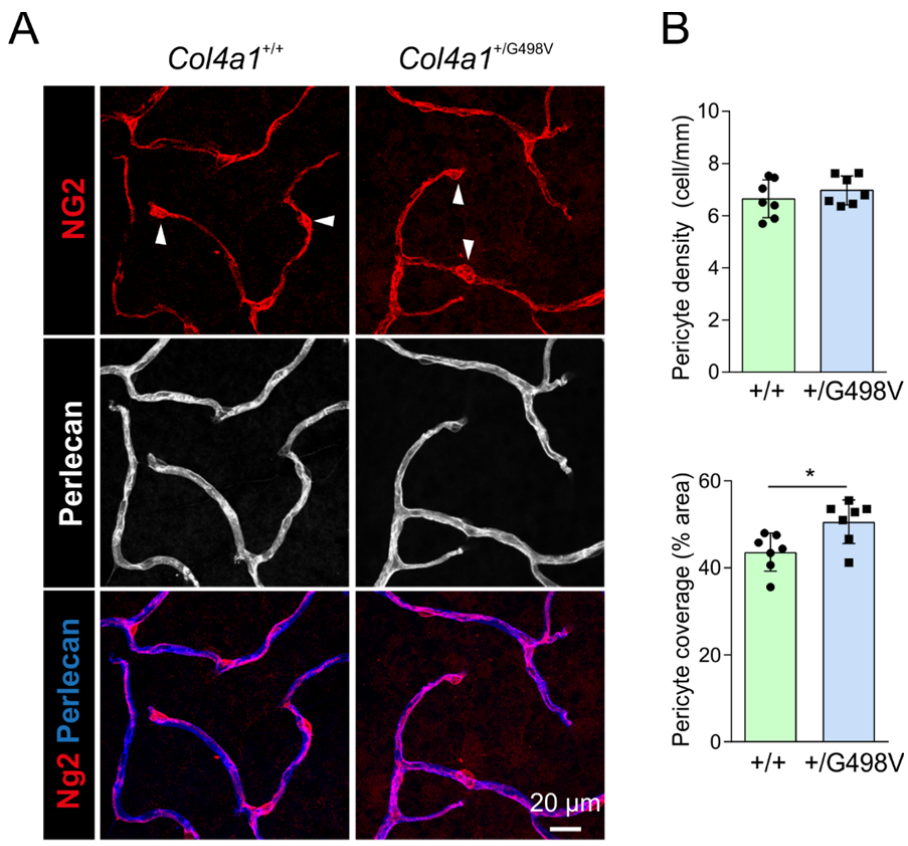

Figure S7

Figure S7. Pericyte coverage in *Col4a1*$^{+/G498V}$ mice.

A. Representative confocal pictures of retinal capillaries from *Col4a1*$^{+/+}$ and *Col4a1*$^{+/G498V}$ mice aged 6 months stained for NG2 and perlecan. Arrowheads show pericyte cell nuclei. **B.** Quantification of pericyte density (top) and pericyte coverage (bottom) (n=7 mice per group). * P=0.0165 by Student's t-test. Scale bar: 20 µm.

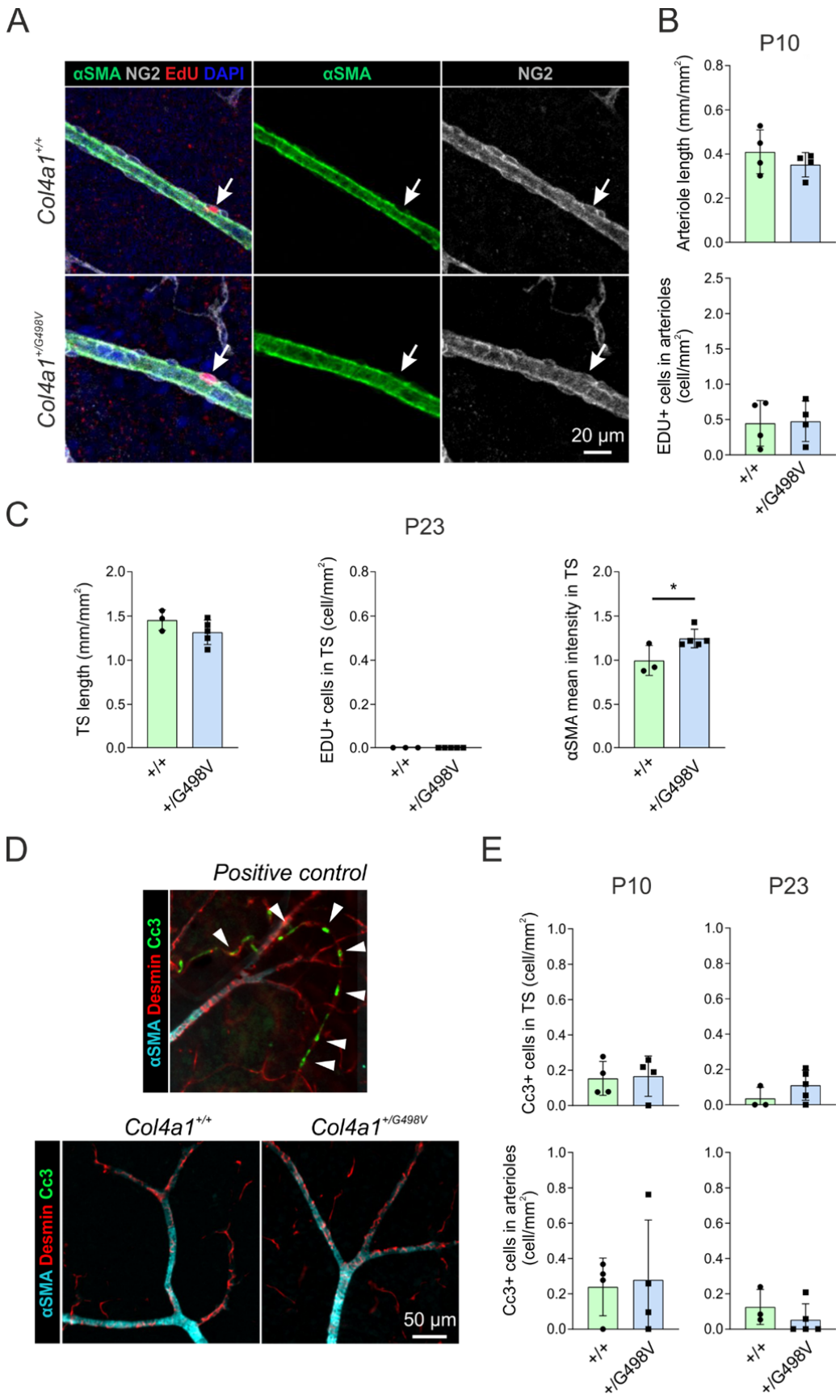
A
αSMA NG2 EdU DAPI
αSMA
NG2
Col4a1+/+
Col4a1+/G498V
20 µm
B
P10
Arteriole length (mm/mm2)
EDU+ cells in arterioles (cell/mm2)
+/+
+/G498V
C
P23
TS length (mm/mm2)
EDU+ cells in TS (cell/mm2)
αSMA mean intensity in TS
*
D
Positive control
αSMA Desmin Cc3
Col4a1+/+
Col4a1+/G498V
50 µm
E
P10
P23
Cc3+ cells in TS (cell/mm2)
Cc3+ cells in arterioles (cell/mm2)

Figure S8

Figure S8*:* Analysis of proliferation and apoptosis of arteriolar SMCs and transitional cells in the developing retina from *Col4a1*$^{+/+}$ and *Col4a1*$^{+/G498V}$ mice

A. Representative confocal images of retinal arterioles from *Col4a1*$^{+/+}$ and *Col4a1*$^{+/G498V}$ mice aged 10 days stained for EdU incorporation (4 hours) together with α-SMA, NG2, and DAPI. Noting the immature aspect of arteriolar SMCs at P10, which are NG2 bright with protruding nuclei. Arrows point to proliferating SMCs. **B**. Quantification at P10 of the relative total length of arterioles (*P*=0.3485) and the relative mural cell proliferation in arterioles (*P*=0.8994) (n=4 mice per group). **C.** Quantification at P23 of the total length of TS (*P*=0.2027) stained for α-SMA, mural cell proliferation in TS and α-SMA mean fluorescence intensity in TS (**P*=0.0388) (n=3 +/+ and 5 +/G498V). **D.** Representative confocal images of retinal vessels of P23 mice stained for cleaved caspase 3 (Cc3) together with α-SMA and desmin. Shown are images of a regressing hyaloid vessel with cleaved caspase 3 positive cells (arrowheads) (positive control, top panel) and images of retinal TS from *Col4a1*$^{+/+}$ and *Col4a1*$^{+/G498V}$ (bottom panel). **E.** Quantification of the number of cleaved caspase 3 positive cells in arterioles and TS from *Col4a1*$^{+/+}$ and *Col4a1*$^{+/G498V}$ at P10 (n=4 mice per group) and P23 (n=3 +/+ and 5 +/G498V). Arterioles: P10 (*P*=0.8398); P23 (*P*=0.3283). TS: P10 (*P*=0.8701); P23 (*P*=0.2414). Data were analyzed by student's t-test. Scale Bars: 20 µm (A) and 50 µm (D).

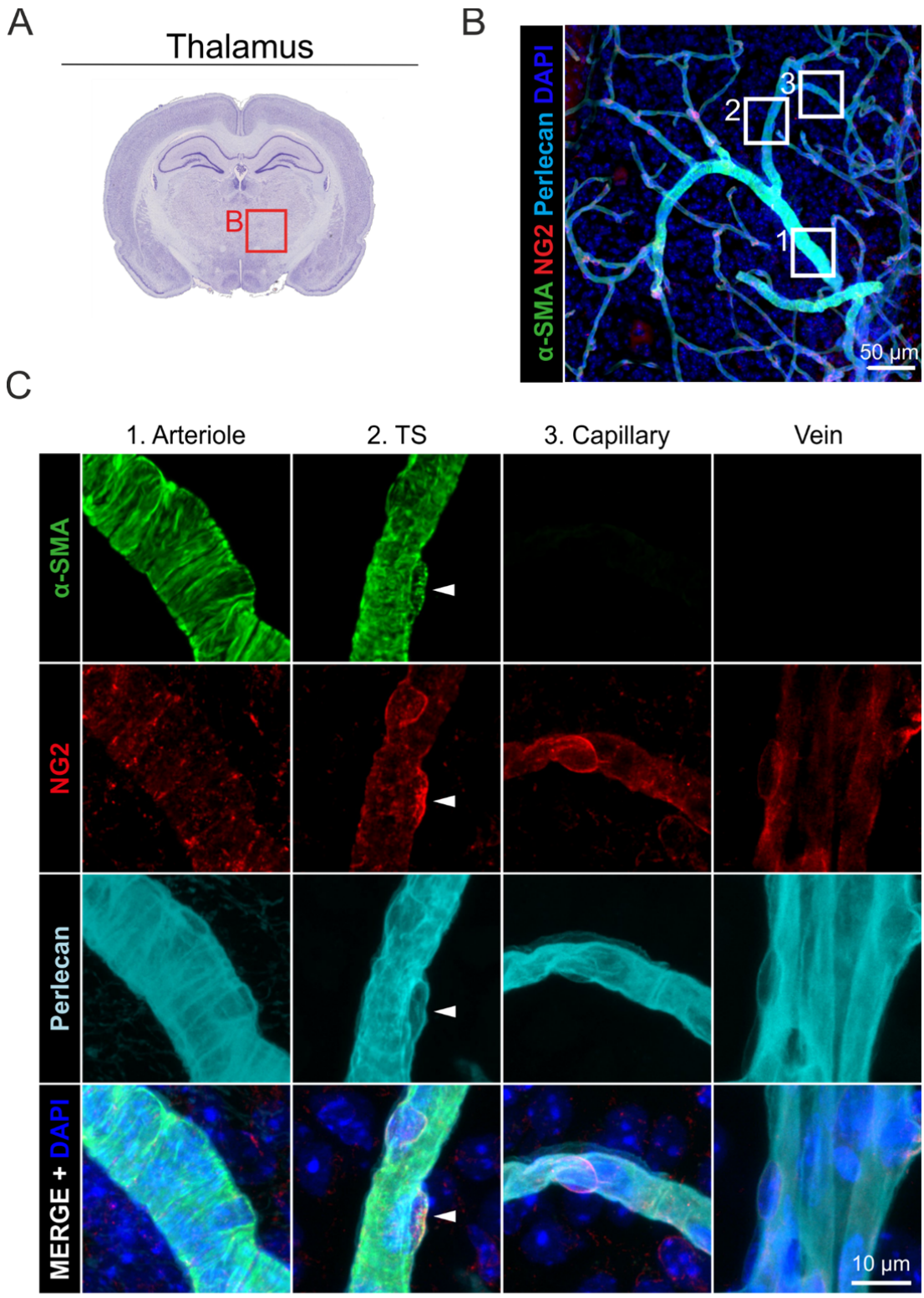

Figure S9

Figure S9: Heterogeneity of mural cells in brain vessels

A. Coronal section of a mouse brain with the thalamus boxed in red. **B-C.** Representative confocal pictures of coronal sections through the thalamus immunostained for α-SMA, NG2, perlecan and DAPI. **C**. Higher magnification pictures of boxed regions numbered in B, showing SMCs in arterioles (1), transitional cells in TS (2), pericytes in capillaries (3) and SMCs in veins. Arrowheads point to protruding nuclei of transitional cells in TS. Scale bars: 50 μm (B) and 10 μm (C).

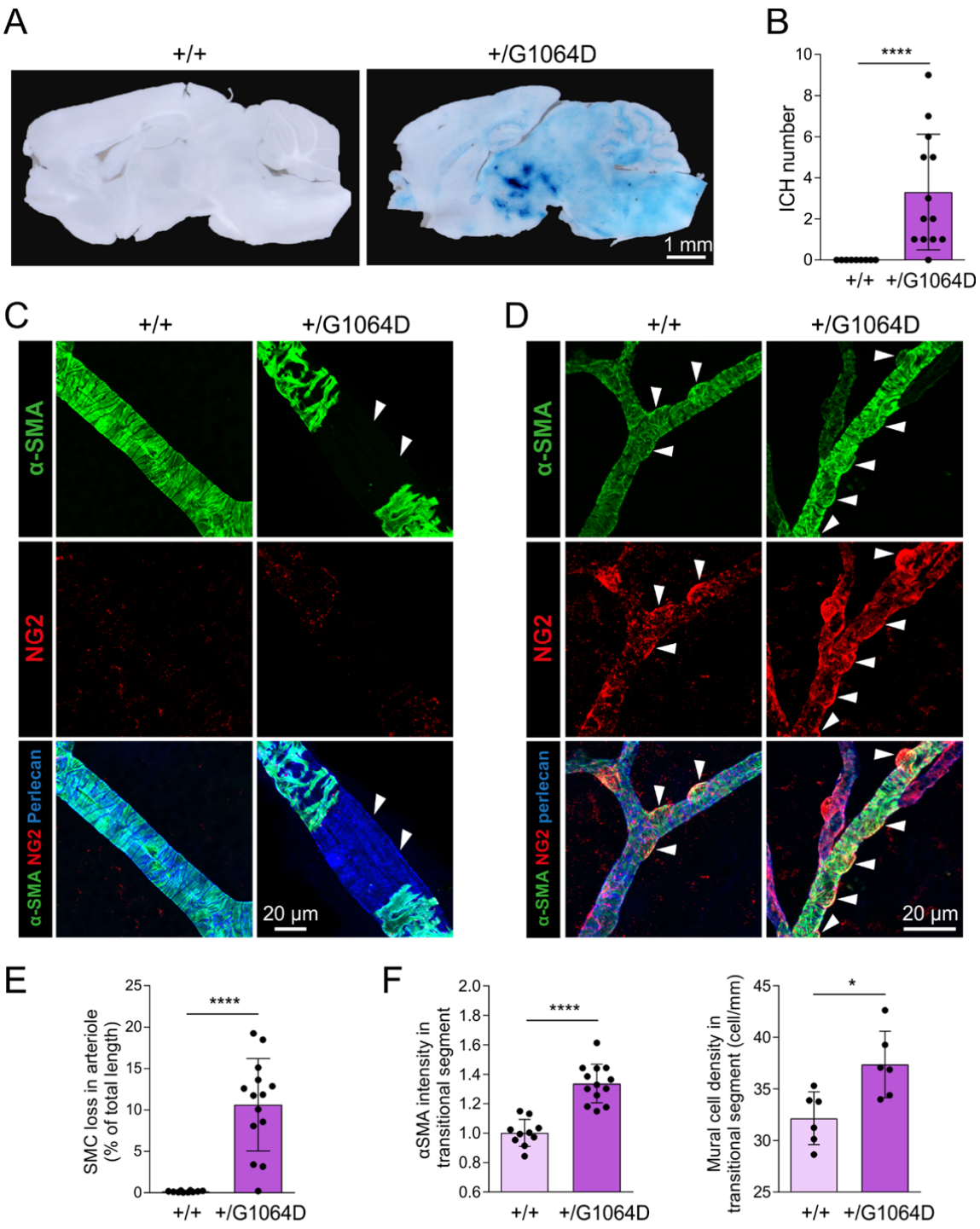

Figure S10

Figure S10: *Col4a1*$^{+/G1064D}$ mice develop spontaneous deep ICH and exhibit both SMC loss in arterioles and exaggerated muscularization of TS in the retina.

A. Representative images of sagittal brain sections stained for hemosiderin (Perl's staining) of *Col4a1*$^{+/+}$ and *Col4a1*$^{+/G1064D}$ mice at 3 months showing deep ICHs in mutants. **B.**

Quantification of the number of ICH in *Col4a1*$^{+/+}$ (n=9 mice) and *Col4a1*$^{+/G1064D}$ (n=13 mice) mice at 3 months. **** P<0.0001 by Mann-Whitney test. **C-D**. Representative confocal pictures of retinal arterioles (**C**) and retinal TS (**D**) from *Col4a1*$^{+/+}$ and *Col4a1*$^{+/G1064D}$ mice at 3 months stained for α-SMA, NG2 and perlecan. Arrowheads show SMC loss (**C**) and increased number of NG2-bright transitional cell bodies (**D**) in mutant mice. **E.** Quantification of SMC loss in retinal arterioles (n=10 *Col4a1*$^{+/+}$ and 14 *Col4a1*$^{+/G1064D}$ mice). **** P<0.0001 by Student's t-test. **F**. Quantification of α-SMA fluorescence intensity (n=10 *Col4a1*$^{+/+}$ and 13 *Col4a1*$^{+/G1064D}$ mice) and mural cell density (n=6 mice per group) in TS. * P=0.0113 **** P<0.0001 by Student's t-test. Scale bars: 1 mm (A) and 20 µm (C, D).

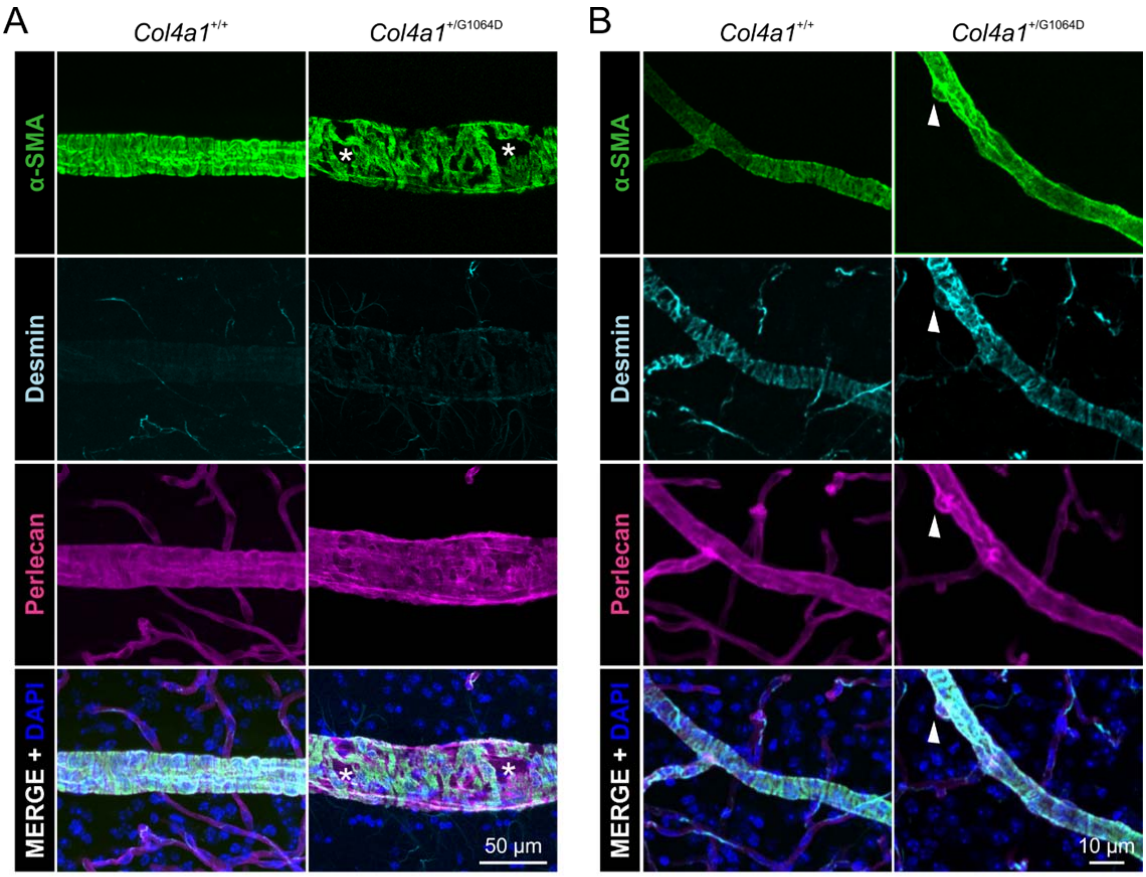

Figure S11

Figure S11. *Col4a1*$^{+/G1064D}$ mice exhibit SMC loss in arterioles and exaggerated muscularization of TS in the brain.

A-B. Representative confocal pictures of brain sections (thalamus) from *Col4a1*$^{+/+}$ and *Col4a1*$^{+/G1064D}$ mice aged 3 months stained for α-SMA, desmin, perlecan and DAPI showing prominent SMC loss (star) with a ballooned aspect in the mutant arteriole (**A**) and hypermuscularization of mutant TS (arrowheads) (**B**). Scale bars: 50 µm (A) and 10 µm (B).

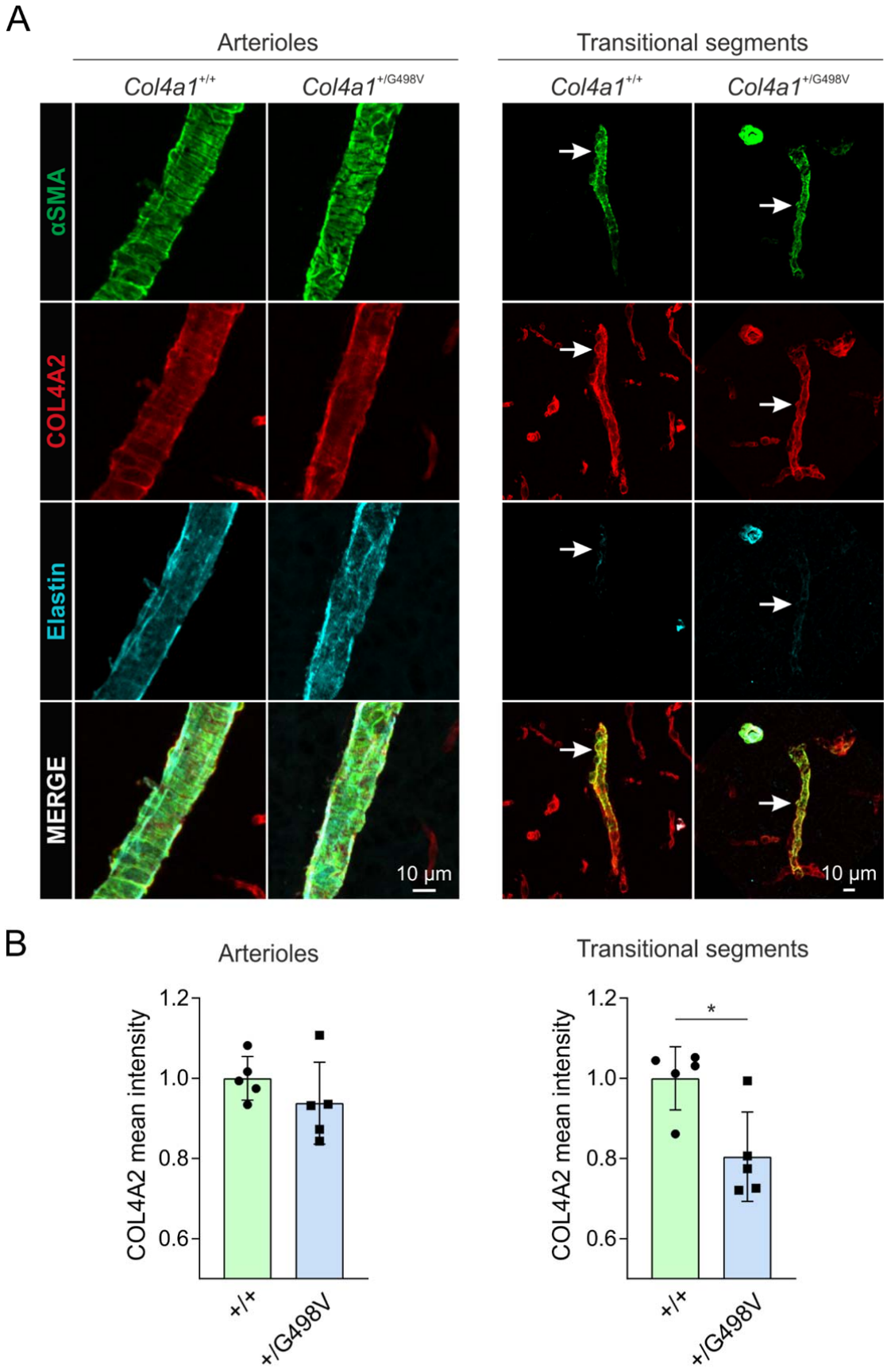
A
Arterioles
Transitional segments
Col4a1+/+
Col4a1+/G498V
Col4a1+/+
Col4a1+/G498V
αSMA
COL4A2
Elastin
MERGE
10 μm
10 μm
B
Arterioles
Transitional segments
COL4A2 mean intensity
1.2
1.0
0.8
0.6
*
+/+
+/G498V
+/+
+/G498V

Figure S12

Figure S12: Brain expression of COL4A2 is decreased in TS but unchanged in arterioles of *Col4a1*$^{+/G498V}$ mice.

A. Representative confocal pictures of brain sections (thalamus) from *Col4a1*$^{+/+}$ and *Col4a1*$^{+/G498V}$ mice aged 6 months stained for α-SMA, elastin and COL4A2 showing unchanged expression of COL4A2 in mutant arterioles and decreased expression in mutant TS (white arrow)—arterioles were identified as vessels positive for α-SMA and elastin, and TS as vessels positive for α-SMA and negative for elastin. **B.** Quantification of COL4A2 fluorescence intensity in cerebral arterioles and TS of *Col4a1*$^{+/+}$ and *Col4a1*$^{+/G498V}$ mice (n=5 mice per group). Arteriole (P=0.2670), TS (* P=0.0125) by Student's t-test. Scale bar: 10 µm.

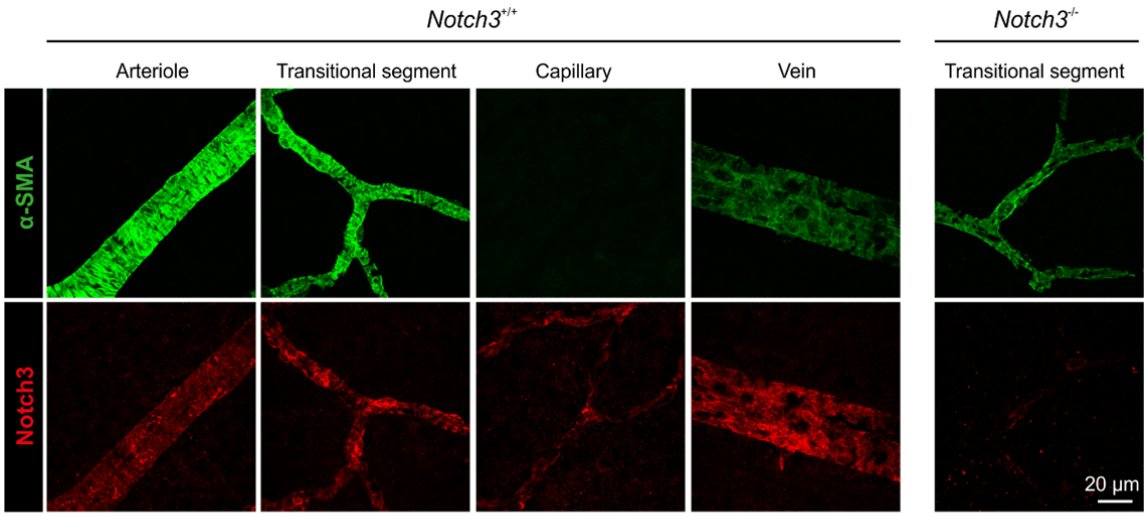

Figure S13

Figure S13: Expression of Notch3 in vascular mural cells.

Representative confocal pictures of retinal vessels from adult mouse stained for α-SMA and Notch3 showing Notch3 expression in SMCs, transitional cells and pericytes. Panel on the right shows lack of Notch3 staining in *Notch3*$^{-/-}$ vessels. Scale bar: 20 µm.

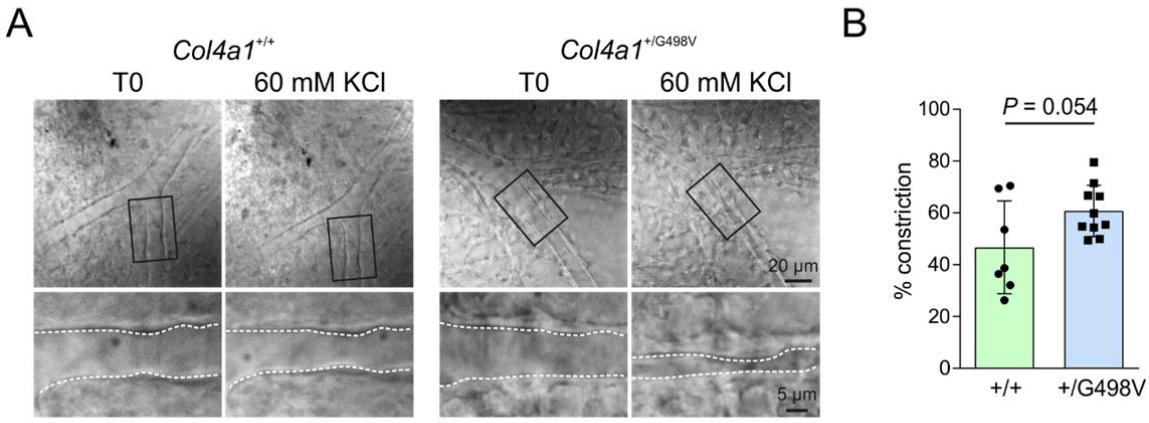

Figure S14

Figure S14. Constriction response of retinal TS to 60 mM KCl.

A. Experiments were done in pressurized retina explants. Bright field images of retinal TS from *Col4a1*$^{+/+}$ and *Col4a1*$^{+/G498V}$ mice at 6 months before (T0) and after addition of 60 mM KCl to the perfusion chamber. Bottom pictures show higher magnification view of the black boxed area. Dashed white lines delineate the vessel wall. **B.** Quantification of the constriction response in *Col4a1*$^{+/+}$ (n=7 mice) and *Col4a1*$^{+/G498V}$ mice (n=10 mice) in the presence of 60 mM KCl. *P*=0.0544 by Student's t-test. Scale bars: 20 µm (A, top) and 5 µm (A, bottom).

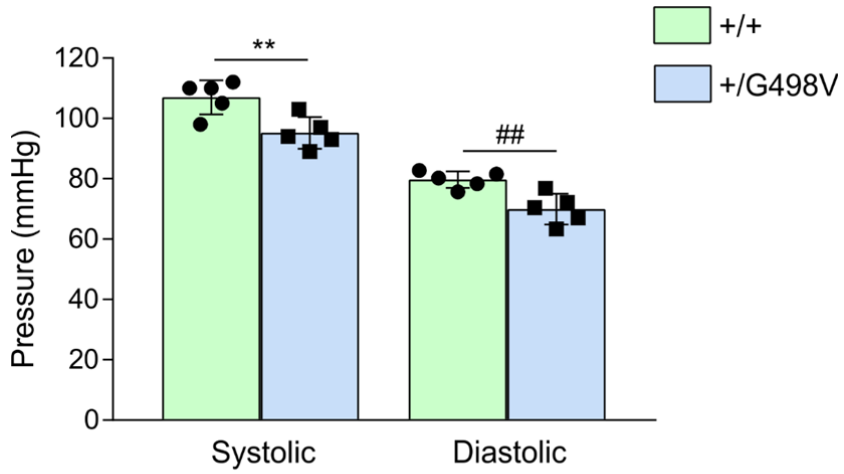

Figure S15

Figure S15. Arterial blood pressure in *Col4a1* mutant mice.

Blood pressure was measured by tail-cuff plethysmography in control and *Col4a1*$^{+/G498V}$ mice aged 6 months (n=5 mice per group). ** P=0.009, ## P=0.0056 by Student's t-test.

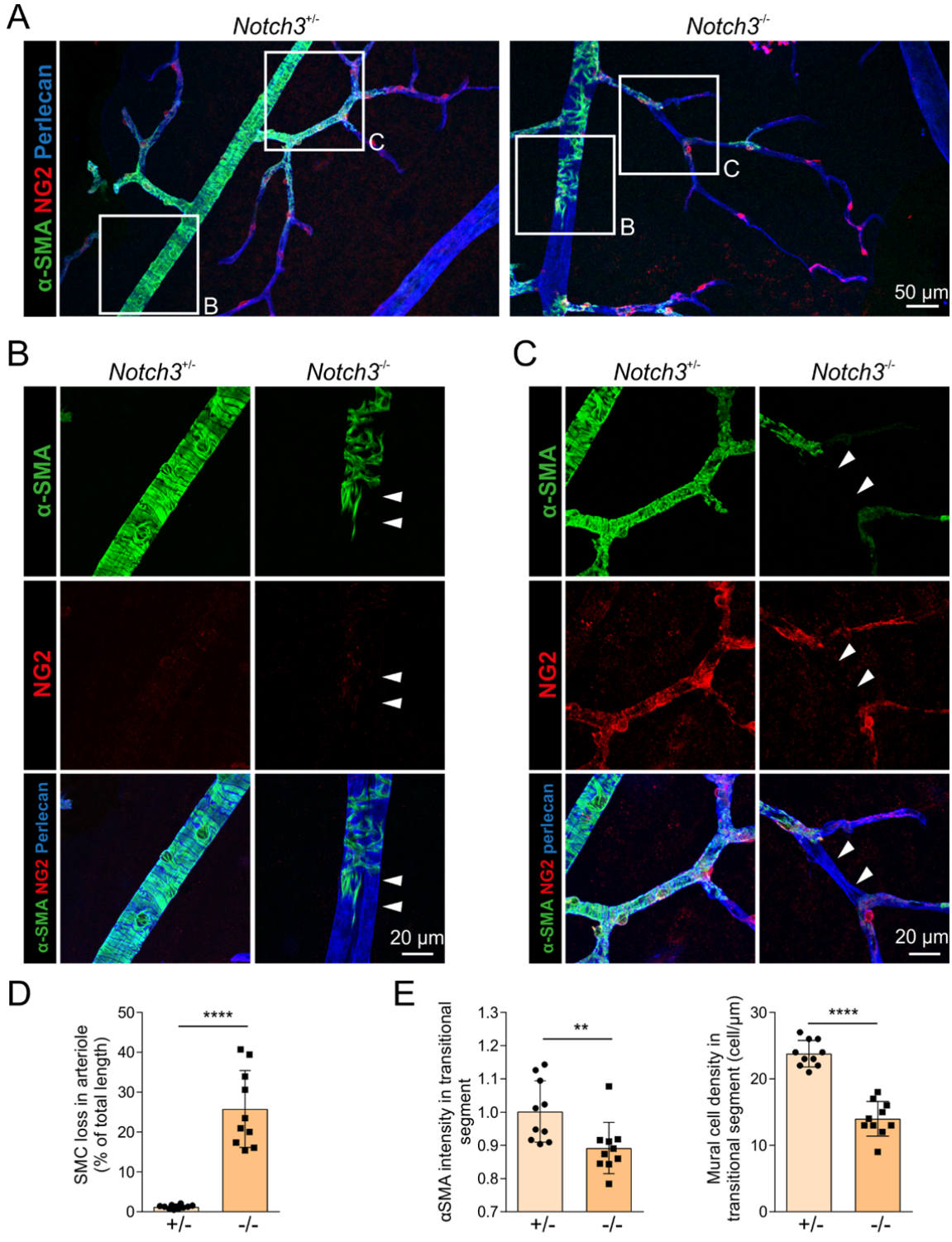

Figure S16

Figure S16. *Notch3*$^{-/-}$ mice exhibit mural cell loss in retinal arterioles and transitional segments.

A. Representative confocal pictures of retinal vessels from *Notch3*$^{+/-}$ and *Notch3*$^{-/-}$ mice at 12 months stained for α-SMA, NG2 and perlecan. Higher magnifications of white boxed areas are shown in B and C. **B**. Arterioles of *Notch3*$^{+/-}$ and *Notch3*$^{-/-}$ mice. Arrowheads point to marked SMC loss in mutant arteriole. **C**. TS of *Notch3*$^{+/-}$ and *Notch3*$^{-/-}$ mice. Arrowheads show pronounced loss of transitional cells in mutant TS. **D**. Quantification of SMC loss in arterioles (n=10 mice per group). **** $P<0.0001$ by Student's t-test. **E**. Quantification of mural cell density and α-SMA fluorescence intensity in TS (n=10 mice per group). ** $P=0.0098$, **** $P<0.0001$ by Student's t-test. Scale bars: 50 µm (A), 20 µm (B, C)

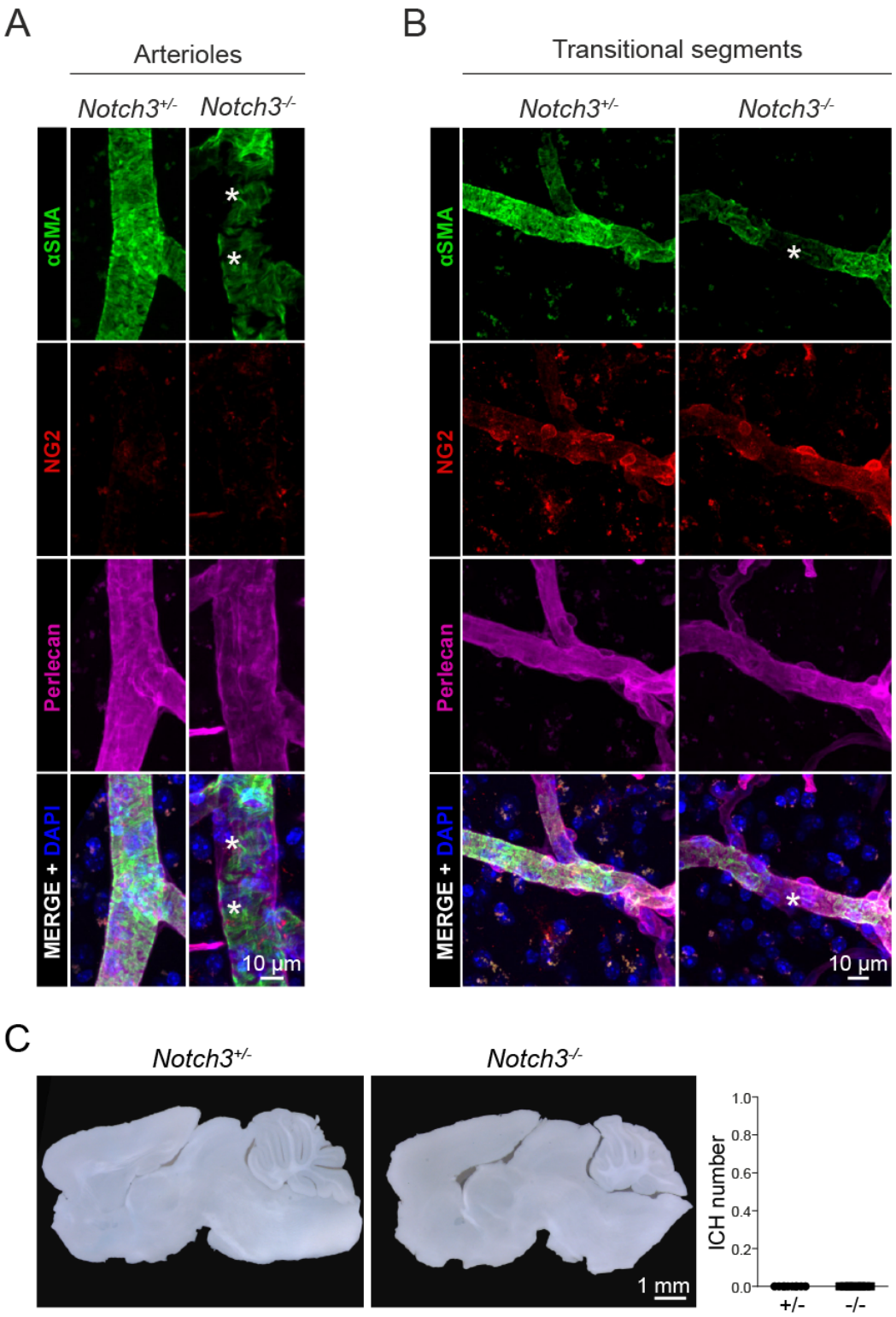

Figure S17

Figure S17. *Notch3*$^{-/-}$ mice exhibit mural cell loss in brain arterioles and TS but do not develop deep ICH.

A, B. Representative confocal pictures of brain arterioles (A) and TS (B) from *Notch3*$^{+/-}$ and *Notch3*$^{-/-}$ mice at 12 months stained for α-SMA, NG2, perlecan and DAPI, showing severe loss of mural cells in both mutant arteriole and mutant TS (stars)—punctate staining outside vessels corresponds to lipofuscin autofluorescence. **B**. Representative sagittal brain sections of *Notch3*$^{+/-}$ and *Notch3*$^{-/-}$ mice at 12 months stained with the Perl's coloration, showing absence of deep ICH. Quantification of ICHs is shown on the right (n=10 mice per group). Scale bars: 10 μm (A, B), 1 mm (C).

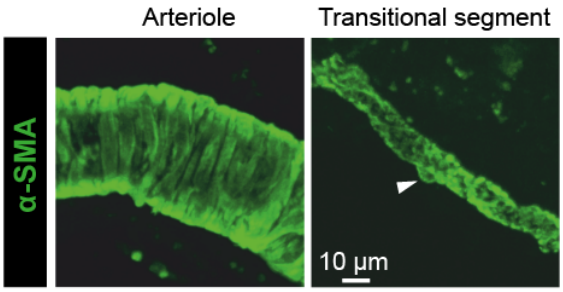

Figure S18

Figure S18. SMCs and transitional cells in human cerebral vessels.

Representative confocal pictures of human cerebral vessels stained for α-SMA showing SMCs in arterioles (left) and transitional cells in TS (right, arrowheads). Scale bar: 10 µm.

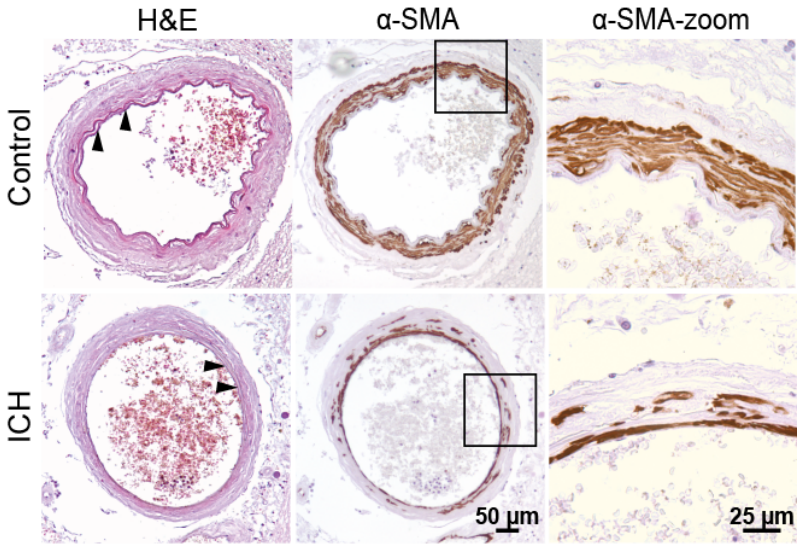

Figure S19

Figure S19. Focal and segmental SMC loss in brain arteries of ICH patients. Representative images of cerebral arteries (basal ganglia) from control and ICH patients stained with hematoxylin and eosin (left) or immunostained for α-SMA (middle and right panels). Pictures on the right panel are higher magnifications of the boxed area in the middle panel showing an artery exhibiting SMC loss in the arterial wall in ICH patients. Shown is a thinner internal elastic lamina in ICH patients (arrowheads). Scale bar: 50 μm (left and middle) and 25 μm (right)

Additional Tables

Supplementary Table 1. Primers used for quantitative RT-PCR shown on Figure 4.

Gene	Forward primer 5'-3'	Reverse primer 5'-3'
Acta2	CCTGGCCTAGCAACACTGAT	GGGGGCCACCCTATAATAAA
Calponin	TTACGGTTTGGGGAGATGAG	TGGAAGGGTTTCTGGTTCTG
Cdh6	GTCTGTGCTGGGAAAGGTGT	CTTGGTTTGGTGTGATGGTG
Desmin	AGAGGTTGTCAGCGAGGCTA	CTTCAGGAGGCAGTGAGGAC
Grip2	GGGCACCAAACGAACTAAGA	CCACACACCAGAAATCCAGA
HeyL	CCCCTCACCCTACTCACCA	GCTTCAACCCAGACCCAAG
Kcna5	TATCATCGGGAGACAGACCAC	CCAGACAGAGGGCATACAGAG
Myocardin	AGCCTCCTTTTGACAGCATC	CCATTCCATTGTTTCCCAAG
Notch3	ATTTGAGGGGTGCTGAAGTG	GAAGGCTGGGACAGAGAGAA
Nrip2	GGGAAGAATGTGTGGAGTGG	GAAGGCAGCAATGAAGAAGC
Pecam	TGCCTTGTTCATGTTGGGTA	TCTCCTGGAACCTCCTTTCA
Pln	CGAAGCCAAGGTCTCCTAAA	TAGCCGAGCGAGTGAGGTAT
S1pr3	TGCCTTATGAACCCTGGAAG	GCCAATGATGGAGCAGAACT
SM22	TCTAATGGCTTTGGGCAGTT	GCAGTTGGCTGTCTGTGAAG
SMMHC	GGCTTCATTTGTTCCTTCCA	CGAGCGTCCATTTCTTCTTC
Susd5	CAGCAGCAGATTGAGATGGA	CTTTAGGCACCCCCAGAGAC
Tbx2	GGCACCTCCTTCTTTCAACA	GCCTGTCTTTTGTGGGGTAG
Xirp1	GGAGGTGATGTTCAGGGCTA	CTGTTGCTCTTGTTGGTGGA
β-actin	CTGCGTCTGGACCTGGCT	ACGCACGATTTCCCTCTCA

Supplementary Table 2: Resting diameters of pressurized transitional segments (40 mmHg) used for experiments described in Figure 6 and S14.

	***Col4a1*$^{+/+}$**	***Col4a1*$^{+/G498V}$**
	9.0 10.6 12.1 8.2 13.5 9.8 10.1	12.9 9.3 10.1 11.2 7.9 9.6 11.4 7.8 6.1 8.4
Mean (µm)	10.5	9.5
SD (µm)	1.8	2.0

Supplementary Table 3: Demographics of individuals whose brain tissues were used for experiments described in Figure 8.

Controls	BBN number	Age	Sex	Death certificate	PM interval (hours)	Neuropathological findings	Hypertension	Anti-hypertensive medication
SD008/17	001.29824	71	F	1a) Ischaemic and hypertensive heart disease 1b) Diabetes mellitus	96	No significant abnormalities	Yes unknown	Yes
SD025/17	001.30208	73	M	1a) Ischaemic heart disease with cardiac enlargement	66	Mild arteriolar CAA Braak tangle stage 1 WM pathology, moderate Moderate non-amyloid SVD	No history	N/A
SD005/17	001.29696	84	M	1a) Sepsis from chronic leg wounds 2) Bullous Pemphigoid, atrial fibrillation, Insulin dependent diabetes	23	Braak tangle stage 1 WM patology, mild Mild non-amyloid SVD	Yes 29 years	Yes
SD012/17	001.29882	71	F	1a) Plastic bag suffocation	95	Braak tangle stage 1 WM patology, mild Mild non-amyloid SVD	No history	N/A
SD046/17	001.31504	65	F	1a) Ischaemic and hypertensive heart disease	76	Thal amyloid phase 1 Braak tangle stage 1 WM pathology, mild Mild non-amyloid SVD	Yes months	Yes
SD021/17	001.30147	67	M	1a) Ischaemic heart disease	68	Thal amyloid phase 5 Mild arteriolar CAA Braak tangle stage 1 WM pathology, mild Moderate non-amyloid SVD	No history	N/A
SD036/17	001.30916	71	M	1a) Haemopericardium 1b) Ruptured myocardial infarct 1c) Coronary artery atheroma and thrombosis	71	Thal amyloid phase 3 Braak tangle stage 2	Yes 8 years	Yes
Deep ICH	**BBN number**	**Age**	**Sex**	**Death certificate**	**PM interval (hours)**	**Neuropathological findings**	**Hypertension**	**Anti-hypertensive medication**
SD022/15	001.26490	63	M	1a) Aspiration pneumonia 2. ICH	28	Tumour Haemorrhage, intracerebral	No history	N/A
SD061/14	001.24531	84	M	1a) ICH	23	Haemorrhage, intracerebral Vascular disease, lacunar	Yes 7 years	Yes
SD026/14	001.22228	73	F	1a) ICH	165	Braak stage 2 CAA, Sporadic Vascular disease, lacunar Haemorrhage, intracerebral	No history	N/A
SD025/14	001.22227	81	M	1a) ICH	27	Haemorrhage, intracerebral Vascular disease, lacunar Tauopathy, unspecified	Yes 2 years	Yes
SD056/13	001.19596	65	M	1a) ICH	36	Haemorrhage, intracerebral Vascular disease, lacunar	No history	N/A

SD043/13	001.19599	67	M	1a) Aspiration pneumonia 1b) ICH 2) Hypertension COPD Alcohol excess	77	Braak stage 2 Haemorrhage, intracerebral Vascular disease, lacunar	Yes 15 years	Yes
SD041/13	001.19601	77	F	1a) ICH 2) MI Bronchiectasis	79	Haemorrhage, intracerebral Vascular disease, lacunar Lewy body disease, brain stem subtype	Yes 9 years	Yes

SVD, small vessel disease; CAA, cerebral amyloid angiopathy, MI, myocardial infarct, WM, white matter